Towards Mobile Data Centres: Provision of End-to-End 10 and 40 Gbit/s Ethernet Train Backbones on International Rolling Stock

Felix Ngobigha, Geza Koczian, and Stuart D. Walker

***Abstract*—The next generation of railway customer-oriented services are expected to generate a large volume of data (≈ 10s of TB). As a result, passengers' applications, safety, security, and Internet-on-Board (IoB) sensors challenge current Train Communication Networks. With the present Ethernet Train Backbone (ETB) specification of just 100 Mbit/s in total, railway passenger services will not support intelligent, seamlessly connected and mobile media on-board trains. In this paper, we propose a novel ETB design with experimental results demonstrating end-to-end 10 Gbit/s and 40 Gbit/s throughput results over existing conducting media on commercial railway carriages. This is equivalent to 100 Mbit/s per user on real-world railway rolling stock and shows that standard RailCat 5e cabling and new rail-approved 10 Gbit/s ETB active nodes (switches) fully support emerging trends and future-proof ETB configurations.**

***Index Terms*—ETB train regions, passive components, active network devices, Ethernet consist network, twisted-quad cable, quadrupole.**

I. Introduction

EFFECTIVE communications have always been identified as one of the essential operational parameters for railway operation. Historically, there have been challenges in terms of non-interoperability. As a result, a set of international standards such as IEC 61375 were developed [1], [2], to overcome this situation namely: the Train Communication Network (TCN) which defines a system architecture and the necessary protocols for communication at train and vehicle level [3] was first introduced. It consists of a Multifunction Vehicle Bus (MVB) [4] inside each carriage and the Wire Train Bus (WTB) [5] to connect the different vehicles. The TCN components have been standardized in IEC 61375 as above. The current TCN configuration comprises the Ethernet Train Backbone (ETB) [6] and Ethernet Consist Network (ECN) [7] with a specification up to 100 Mbit/s with physical links along the train to connect the active network devices together. This is perceived as inadequate, for example, a 500 passenger train would offer just 200 kbit/s per passenger. Providing a rich movie experience such as H.265 real-time 4K video streaming at 15 Mbit/s for 500 passengers requires 7.5 Gbit/s. Even higher loads are possible noting that 130 - 180 passengers for 9 carriages during peak periods [8], [9] will consume 24.3 Gbit/s. This introduces a massive challenge to the train operating companies (TOCs) and forms the motivational basis for this work. Without the ultra-high capacity ETB described here, advances in train-to-shore 5G wireless (for example) and beyond will be neutralized [10]–[12]. Various technologies for inter-carriage connection such as millimetre wave (mmWave) radio, optical wireless, and fibre-optic communication [13]–[18] have all been considered for ETB applications. However, these have performed badly in the harsh railway environment, for example: wide temperature range, humidity, electromagnetic interference, water ingress, abrasive substances, and large-scale mechanical misalignment due to carriage sway and track curvature.

Prior to this study, ETB realization used standard conducting media technologies which were limited to 100 Mbit/s maximum due to inappropriate cable and connector provision. These fell far short of the seamless higher data rate connectivity required for on-board operation related-services and active users. Due to environmental barriers and sensitivity to blockages and shadowing at higher frequencies as with mmWwave, the radio link between carriages must be carefully designed to counter non-line-of-sight (NLOS) situations, typically by using beam forming techniques [19]. Using the subset of optical wireless communications technologies [20] such as visible light communication (VLC) and free space optics (FSO) for ETB has also shown susceptibility to atmospheric conditions such as fog and dust. Additionally, the unquestioned capacity of fibre-optic cables in communication systems together with low power loss, and immunity to electromagnetic interference has to be weighed against the harsh abrasive railway environment.

A discussion around future railway services and bandwidth requirements was presented [14] based on lower frequency wireless technologies, including inter-carriage connection based on IEEE802.11 [21], WiMAX [22], [23] with dedicated short-range communications [18]. Guan et al [14] also pointed out the difficulty of accurately analyzing the on-board bandwidth with respect to the number of active users during peak period, simultaneous communication within certain scenarios, and different service types. In summary, we show here that the provision of end-to-end, future-proof ETB

Manuscript received mm/dd/yyyy; revised mm/dd/yyyy. (Corresponding author: Felix Ngobigha).

F. Ngobigha is with the Digital Futures Institute (DFI) in the School of Technology, Business and Arts (formerly known as School of Engineering, Arts, Science, and Technology), University of Suffolk, Neptune Quay, Ipswich, IP4 1QJ, United Kingdom, E-mail: f.ngobigha@uos.ac.uk.

G. Koczian and S. D. Walker are with the Access Network Group (ANG) in the School of Computer Science and Electronic Engineering, University of Essex, Wivenhoe Park, Colchester, CO4 3SQ, United Kingdom, E-mail: gkoczi@essex.ac.uk, and stuwal@essex.ac.uk.

physical layers on international rolling stock calls for robust and reliable very high capacity links which include retrofit opportunities on future railway passenger-related services. In this paper, we comprehensively revisit the design, implementation and evaluation of existing ETBs while adhering to the severe constraints on connectors and cabling provision. Use of classical electromagnetic field and transmission line theory resulted in an ETB based on internally–modified standard connector shells and rail-approved cabling such that error-free, end-to-end train throughputs of 10GbE and 40GbE were measured on existing train retrofit. This represents up to 400 times improvement on the original l00 Mbit/s capacity with opportunities for 100GbE. It is suggested that trains of the future could become mobile data centres for their passengers. This rigorous approach has led to a significant reduction of crosstalk issues which meant ensuring inter-pair shielding for multi-pair cables and secondly, cabling and connectorisation at gigabit data rates while retaining compliance with standard.

This paper is structured as follows: In Section II, we present the physical layer model for the 10 Gbit/s and 40 Gbit/s ETB, following a quadrupole design as outlined in [24]. Section III encompasses the implementation, evaluation and experimental numerical results discussion. Finally, section IV provides concluding remarks summarizing the findings and future work.

II. ETB Physical layer model

In this section, the design principles of the proposed ETB physical layer model are presented based on [24] and determine the feasibility of utilizing passive guided media methods to achieve higher data rates in retrofit and future railway passenger-oriented services. The main requirements are to minimise crosstalk/electromagnetic interference within the connectors, reduce termination issues for RailCat 5e cable, and avoid using 4 x 8-wire braided Shielded Foil Twisted-Pair (S/FTP) cabling for the ETB physical layer of the train regions such as inter-car and inter-consist.

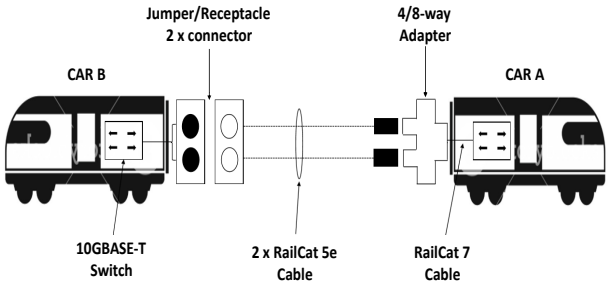

Fig. 1. A sectional schematic of the ETB configuration design with corresponding standard twisted quad/pair copper cables and connectors.

The schematic of the ETB configuration design with corresponding standard RailCat 5e twisted-quads for the Inter-car and/or Inter-consist with the connectors and RailCat 7 within the rolling stock as shown in Figure 1. This assembly in real-world applications have proven to be successful in terms of seamlessly supporting ETB physical layer link speed of 10 Gbit/s. The receptacle is a contact device installed at the outlet for the connection of an attached plug (known as a Jumper in rolling stock industry parlance). The rail-approved connector design does not adequately account for electromagnetic shielding and crosstalk between neighbouring pairs of the four pins; such crosstalk being at variance with IEEE 802.3an (10GBASE-T) standards [25]. Based on the intuitive analysis of the pins connector in terms of electromagnetic interference and crosstalk, it became apparent that the configuration is similar to an electromagnetic non-collinear dipole pair (quadrupole) as discussed [26]. The requisite arrangement was initially applied to a section (2 x 4-wire RailCat 5e twisted-quad cables) and terminated onto 2 x rail-approved connectors by employing this quadrupole configuration based on balanced/symmetrical fields on the four pins termination. This minimizes the effect of crosstalk between cable quads with equal and opposite fields having a cancellation effect. Alternatively, since the next improvement is expected to be four times higher in throughput, the configuration was changed slightly in contrast to the approach described in [24] by utilizing an arrangement of 8 x 4-wire RailCat 5e twisted-quad copper cables as the inter-consist or inter-car Jumper system with careful consideration to reducing the effect of alien crosstalk (which occurs when cable bundles run in close proximity). The RailCat cables cross-sections used for this experiment are shown in Figures 2 and 3.

Fig. 2. Cross-section of a typical 8-wire RailCat 7 twisted-pair cable with seven conductor strands

Fig. 3. Cross-section of a typical 4-wire RailCat 5e twisted-quad cable with nineteen conductor strands

In constructing the new ETB for the intended applications, the RailCat 5e twisted-quad cable conductors blue and white denote TD+ and TD- respectively are used for transmitting, while the conductors yellow and orange represent RD+ and RD- respectively used for receiving, where TD+ represents transmit data positive-going differential signal, TD- is a transmit data negative-going differential signal, RD+ represents the received data positive-going signal and RD- is a receive data negative-going differential signal. Ideally, the RailCat 5e twisted-quad is designed to support a nominal data rate of 100 Mbit/s and Table I specified data rates for different twisted copper cables with maximum length [27] and [28]. In contrast to the standard enterprise twisted-pair copper cables design, most of the RailCats are ruggedised to suit the harsh railway environment. Comparison of the different RailCat cables used in this experiment for the railway Jumper applications in terms of the dynamic test with the numerical results are shown in Table II.

TABLE I
COMPARISON OF TWISTED COPPER CABLE BASED ETHERNET PHYSICAL (PHY) MEDIUM CHARACTERISTICS

Standard	**Nominal Speed (Mbit/s)**	**Pairs reqd.**	**Cable require-ment**	**Max. Cable length (m)**	**Bandwidth (MHz)**
802.3u	100	2	Cat 5e	100	100
802.3ab	1,000	4	Cat 5e	100	100
802.3an	10,000	4	Cat 6A	100	500
ISO/IEC 11801	10,000	4	Cat 7	100	600

TABLE II
DYNAMIC (FLEXING) APPLICATION TEST RESULTS OF RAIL-APPROVED CABLES FOR THE IMPLEMENTATION OF THE INTER-CONSIST OR INTER-CAR CABLING

Cable	**Cable Construction**	**Cycles to Failure (CF)**		
		$\min_{CF}$	$\max_{CF}$	% diff
Cat 6A	4 x [2 X 0.20 mm^2 (24 AWG)]	3,250	30,000	80
Cat 7	4 x [2 X 0.20 mm^2 (24 AWG)]	1,330	27,895	92
Cat 5e	4 x 0.33 mm^2 (22 AWG)	27,500	66,700	42
Cat 5e	4 x 0.5 mm^2 (20 AWG)	88,000	132,500	20

Considering the results from the dynamic test conducted with different cable construction as shown in Table II, we evaluated the cycles to failure difference as:

$$CF_{\text{diff}}(\%) = \left(\frac{\max_{CF} - \min_{CF}}{\max_{CF} + \min_{CF}}\right)\%. \tag{1}$$

The flexing test results tabulated in Table II shows the limit for performance and reliability to evaluate the mechanical fracturing properties of the sample RailCAT cables. Likewise, the empirical rule [29] was used to determine whether a given data set is normally distributed and to find outliers, which may be the result of experimental errors. As shown in Table II, the RailCat 5e twisted-quad construction with the 20 AWG is preferred for the intended applications of inter-car and/or inter-consist in the ETB train region and has a larger cycles to failure. While there is standard for the RailCat cabling, ETB face unique challenges when managing electrical properties and other factors. Without proper planning, applications could experience many issues, including disrupted network communication and/or inaccurate performance. Therefore, it is necessary to understand the implementation requirements needed for a given application to select a suitable cable for the ETB inter-car and inter-consist region. Furthermore, the flexing test cycling rate for this work was also increased from 15 cycles per minute as implemented in [24] to 20 cycles per minute, this value is considered as a worst case scenario in terms of the carriage sway at maximum speed $\geq$ 250 km/h, achieved by Eurostar trains on the HS1 line between London and the Channel Tunnel [30].

A. Quadrupole analysis

In accomplishing minimal interference within the pins connector, it emerged that the optimum configuration is similar to an electromagnetic quadrupole [26], [31]. We consider a finite length of 4-wire RailCat 5e twisted-quad copper cabling for the ETB train region of inter-car and inter-consist, stripping back considerable length of conductors and terminated onto the connector. This approach will be very relevant in the implementation of the electromagnetic quadrupole and has been discussed in transmission quadrupole mass spectrometer (filter) which historically proved to be very successful in detecting only ions of a certain mass-to-charge ratio particles [32]–[34]. In [26], we noticed that, if all the charges are distributed along an axis (the z-axis for example in a linear quadrupole), then $\cos\hat{i}x = \cos\hat{j}y = 0$, and $\cos\hat{k}z = 1$. In the case of non-collinear discrete charge points, the symmetry axes are as shown in Figure 4. It is assumed that the transmitting pair denotes $+$ve charges while the receiving pair represent $-$ve charges for the quadrupole analysis.

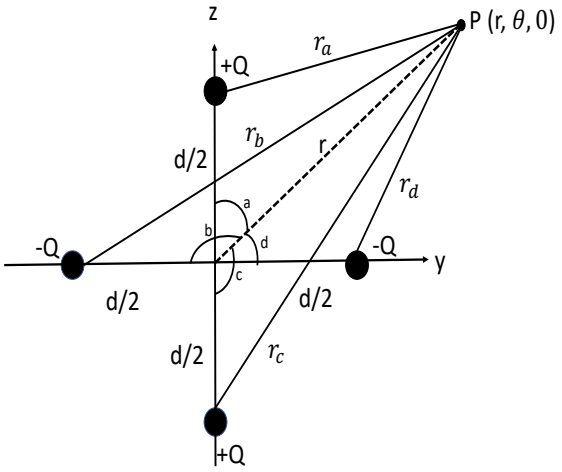

Fig. 4. Configuration of non-colinear quadrupole with discrete charges at y-z plane for the termination of RailCat 5e onto connectors

The analysis started by defining the angles in Figure 4 relative to point $\mathbf{P}(r, \theta, 0)$:

$$\begin{aligned} a &= \theta; \qquad & b &= \frac{\pi}{2} + \theta \\ c &= \pi - \theta; \qquad & d &= \frac{\pi}{2} - \theta, \end{aligned} \tag{2}$$

where **P** is an arbitrary field point. Considering Coulomb's Law, if the localized charge distribution has a net electric charge Q_{net} at far distance, then potential $V(\bar{r})$ to a good approximation will behave very much like that of a point charge:

$$V_{far}(\bar{r}) = \frac{1}{4\pi\epsilon_0}\frac{Q_{net}}{r} \tag{3}$$

and

$$\bar{\mathrm{E}}_{far}(\bar{r}) = -\nabla V_{far}(\bar{r}) = -\frac{1}{4\pi\epsilon_0}\frac{Q_{net}}{r^2} \tag{4}$$

where $1/4\pi\epsilon_0 = K$ is the Coulomb constant. Using the Law of Cosines [35]:

$$c^2 = a^2 + b^2 - 2ab\cos\theta, \tag{5}$$

the source charge locations for the charges with respect to **P** are given as:

$$\begin{aligned} r_a^2 &= \left(\frac{d}{2}\right)^2 + r^2 - 2\left(\frac{d}{2}\right) r\cos\theta \\ &= r^2 + \left(\frac{d}{2}\right)^2 - dr\cos\theta, \end{aligned} \tag{6}$$

$$\begin{aligned} r_b^2 &= \left(\frac{d}{2}\right)^2 + r^2 - 2\left(\frac{d}{2}\right) r\cos(\frac{\pi}{2} + \theta) \\ &= r^2 + \left(\frac{d}{2}\right)^2 + dr\sin\theta, \end{aligned} \tag{7}$$

$$\begin{aligned} r_c^2 &= \left(\frac{d}{2}\right)^2 + r^2 - 2\left(\frac{d}{2}\right) r\cos(\pi - \theta) \\ &= r^2 + \left(\frac{d}{2}\right)^2 + dr\cos\theta, \end{aligned} \tag{8}$$

and

$$\begin{aligned} r_d^2 &= \left(\frac{d}{2}\right)^2 + r^2 - 2\left(\frac{d}{2}\right) r\cos(\frac{\pi}{2} - \theta) \\ &= r^2 + \left(\frac{d}{2}\right)^2 - dr\sin\theta. \end{aligned} \tag{9}$$

Inferring to a point charge of equation (3), the total potential of the configuration can be evaluated using the principle of superposition:

$$V_{quad}(\vec{r}) = V_{+r_a}(\vec{r}) + V_{-r_b}(\vec{r}) + V_{+r_c},(\vec{r}) + V_{-r_d}(\vec{r}), \tag{10}$$

substituting equations (6) - (9) into equation (10) gives:

$$\begin{aligned} V_{quad}(\bar{r}) = &\frac{QK}{r\sqrt{1 + \left(\frac{1}{4}\right)\left(\frac{d}{r}\right)^2 - \left(\frac{d}{r}\right)\cos\theta}} \\ &- \frac{QK}{r\sqrt{1 + \left(\frac{1}{4}\right)\left(\frac{d}{r}\right)^2 + \left(\frac{d}{r}\right)\sin\theta}} \\ &+ \frac{QK}{r\sqrt{1 + \left(\frac{1}{4}\right)\left(\frac{d}{r}\right)^2 + \left(\frac{d}{r}\right)\cos\theta}} \\ &- \frac{QK}{r\sqrt{1 + \left(\frac{1}{4}\right)\left(\frac{d}{r}\right)^2 - \left(\frac{d}{r}\right)\sin\theta}}. \end{aligned} \tag{11}$$

It is worth noting that this is not an approximate mathematical expression for potential associated with pure physical non-collinear quadrupole with charges separated from each other by an equal distance (d) along the y-z plane. Careful choice of coordinate system simplified the mathematics and clarified the physical foundations of the configuration. We reiterate, briefly the development of the electric potential and field intensity for the quadrupole as set out in [26] and [31]:

$$V_{quad} = \frac{1}{4\pi\epsilon_0}\left(\frac{1}{|\mathbf{r}|^3}\right)\sum_{ij}\frac{1}{2}\mathbf{Q}_{ij}n_i n_j \tag{12}$$

where **r** is a vector with origin in the system of charges and n is the unit vector in the direction of **r**. The factors n_i, n_j are components of the unit vector from the point of interest to the location of the quadrupole moment tensor $(\mathbf{Q})$ is a rank-two tensor - 3x3 matrix. For a discrete system of point charges, each with charge Q_l, relative to the coordinate system origin

$\vec{r_l} = (r_{yl}, r_{zl})$, the components of the $\mathbf{Q}$ matrix are defined by:

$$\mathbf{Q}_{ij} = \sum_l Q_l \left(3r_{il}r_{jl} - |\vec{r_l}|^2\delta_{ij}\right), \tag{13}$$

where the indices i, j run over the $y-z$ plane and δ_{ij} is the Kronecker delta [36].

As with any multipole moment, if a lower-order, monopole or dipole, in this case, is non-zero, then the value of the quadrupole moment depends on the choice of the coordinate origin. In our approach to terminating the connectors as shown in Figure 4, we expected that the quadrupole moment will be reduced to zero and coordinate dependent. The associated electric fields can be evaluated using the potential field approach [37] and [38]:

$$\mathbf{E}_{quad} = -\nabla V_{quad}. \tag{14}$$

The negative sign in equation (14) is arbitrary but has been chosen to conform with the convention which directs the vector $\mathbf{E}_{quad}$ outward from a positive discrete charge, and in spherical coordinates form:

$$\mathbf{E}_{quad} = \mathbf{E}_r + \mathbf{E}_\theta + \mathbf{E}_\phi = -\nabla V_{quad}. \tag{15}$$

Explicitly writing out the form of the electric field intensity $\mathbf{E}_{quad}$ for an electric quadrupole with coordinate dependent gives:

$$\begin{aligned}\mathbf{E}_{quad} &= \frac{3\cdot 2Qd^2}{4\pi\epsilon_0}\left(\frac{1}{r^4}\right) \\ &\times \left[\left(\frac{3\cos^2\theta - 1}{2}\right)\hat{r} + \sin\theta\cos\theta\hat{\theta}\right],\end{aligned} \tag{16}$$

where

$$\left(\frac{3\cos^2\theta - 1}{2}\right) = P_n(x)$$

are legendre polynomials of degree 2 with no $\phi-$dependence because the charge configuration is manifestly axially symmetrical in the y-z plane (invariant under arbitrary ϕ rotation). If we assumed that the value of $\theta = 0$, then (16) becomes

$$\mathbf{E}_{quad} = \frac{3\cdot 2Qd^2}{4\pi\epsilon_0}\left(\frac{1}{r^4}\right)\hat{r}. \tag{17}$$

With this analysis, the anticipated bottleneck as a result of the crosstalk within cable and the electromagnetic interference from cables in close proximity has been minimised with improved system performance and higher throughput acheived for the intended applications.

B. Simulation of quadrupole potential and electric field

Other than the quadrupole theoretical analysis of the selected components such as connectors and cables dedicated to the Ethernet. We simulate the quadrupole potential and electric field intensity by assuming four discrete charges, equal magnitude, alternating signs at some distance as shown in Figure 4 which is similar to the configuration described [24]. Evaluation of equation (12) is carried out by adapting the MATLAB code designed for the simulation of a pure, linear (i.e. axially/azimuthally symmetric) electric quadrupole with the moment oriented along the z-axis and using MATLAB version 9.6 R2019a on a 64-bit machine. Figures 5 to 7 show an example of a RailCat 5e cable terminated onto a connector to evaluate the electric potential in three and two-dimensions corresponding to the arrangement of Figure 4.

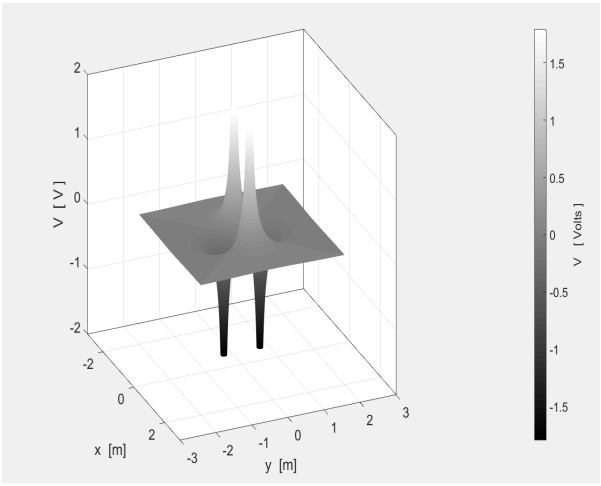

Fig. 5. 3D quadrupole potential of four charges, equal magnitude and alternating signs

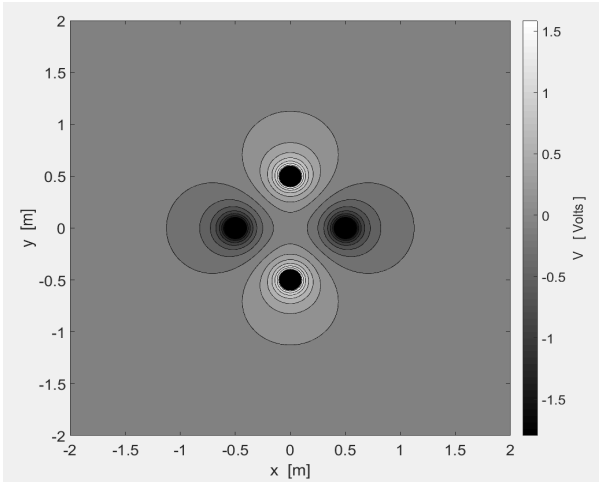

Fig. 6. 2D quadrupole potential of four charges, equal magnitude and alternating signs

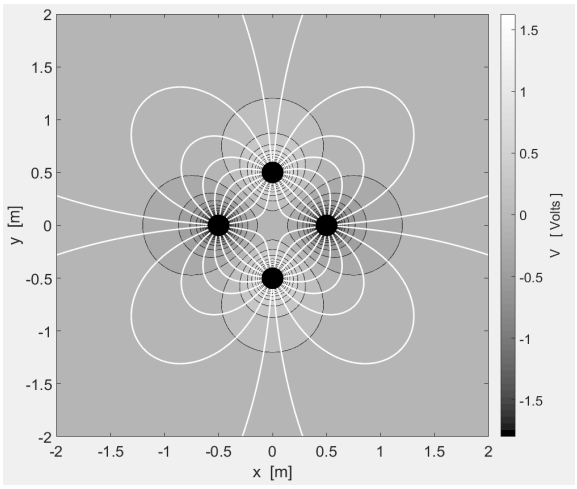

Fig. 7. 2D quadrupole potential of four charges, equal magnitude and alternating signs with field lines

Numerical analysis of the quadrupole electric field intensity of equation (17) is also undertaken following the above approximation where the RailCat 5e cable is terminated onto a connector is shown in Figure 8 also suggests similar patterns is achieved.

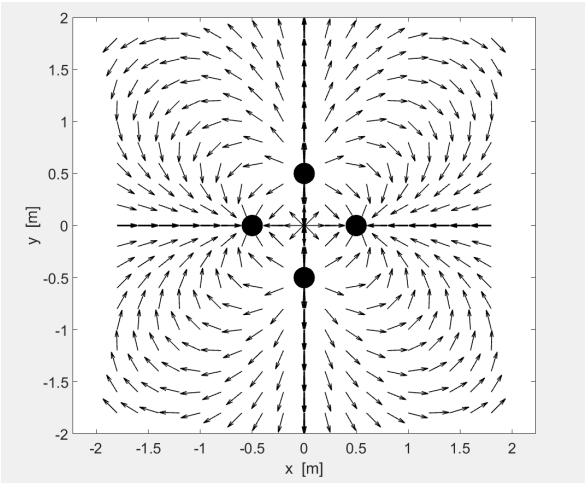

Fig. 8. Quadrupole electric field intensity of four charges, equal magnitude and alternating signs with directions

III. Numerical Results and Discussion

A. Field tester summary results

The summary field tester results using the Fluke Networks CableAnalyzer DSX-8000 for each section of the configuration followed a similar pattern. Satisfactory results were obtained for Transverse Conversion Loss (TCL) which validates how balanced the termination with respect to the RailCat 5e cable and the enhanced connector. Near End Cross Talk (NEXT), Return Loss and Insertion Loss headroom worst-case margins on both the main and smart remote units of the Fluke tester were satisfactory. Obviously, the results were well above the minimum requirements as specified in IEEE 802.3an (10GBASE-T) standards for each section and demonstrated the robustness of our new approach to provide the needed bandwidth at 10 and 40 Gbit/s ETB physical layer speed. The Telecommunications Industry Association (TIA) test limits used in the validation process are more stringent compared with the IEEE 802.an specification.

TABLE III
Summary Fluke Networks CableAnalyzer DSX-8000 results for each section

Test limit	TCL (dB)	NEXT (dB)	Return Loss (dB)	Insertion Loss (dB)	Test status
TIA Cat 6A	41.6	8.2	10.6	45.0	Pass
TIA Cat 6A	41.8	10.0	11.3	44.8	Pass
TIA Cat 6A	40.6	5.4	10.7	44.9	Pass
TIA Cat 6A	40.9	8.1	9.0	44.7	Pass

The numerical results tabulated in Table III for the TCL, NEXT, and Return Loss are shown in terms of worst case margins respectively. While the Insertion Loss values are evaluated with respect to loss margin as tabulated in Table III. The experimental results presented in Table III considering the TIA Channel Cat 6A test limits are in good agreement and follow similar pattern as given in [24]. Figures 9 - 11 are extracted graphs which suggest that the new ETB configuration clearly exceeds the threshold in accordance with TIA Channel 6A test limits.

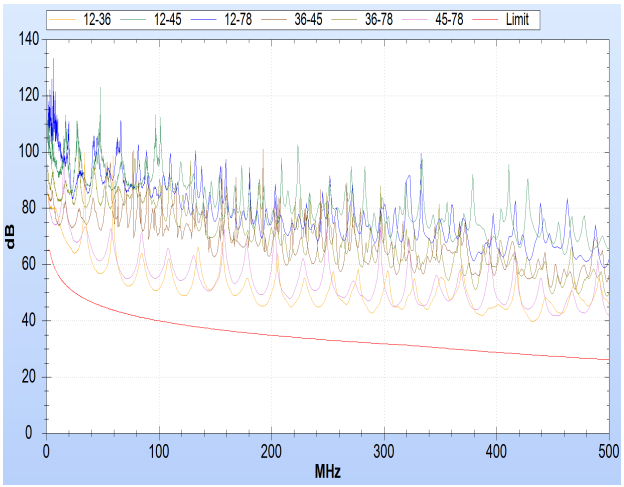

Fig. 9. NEXT of the complete ETB configuration

Taking into consideration the NEXT as a measure of the difference in signal strength between a disturbing pair and a disturbed pair, a larger number (less crosstalk) is more desirable than a smaller number (more crosstalk). Because NEXT varies significantly with frequency, it is important to measure it across a range of frequencies. In broad terms, the NEXT in Figure 9 has a characteristic that varies up and down significantly, while generally increasing in magnitude. This is because twisted-quad coupling becomes less effective for higher frequencies which follows a similar pattern in comparison with that of a twisted-pair.

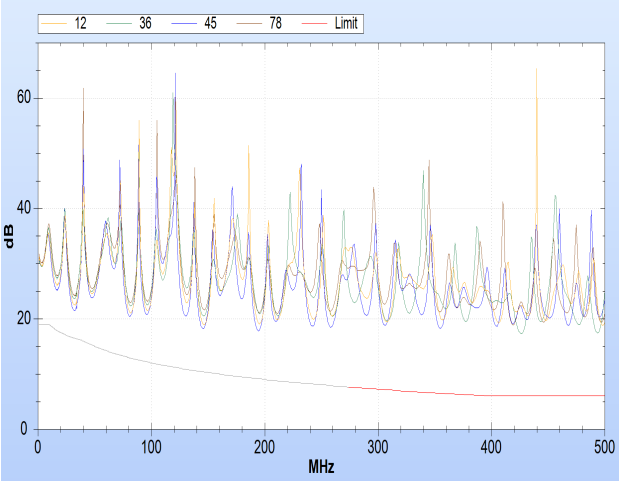

Fig. 10. Return Loss of the complete ETB configuration

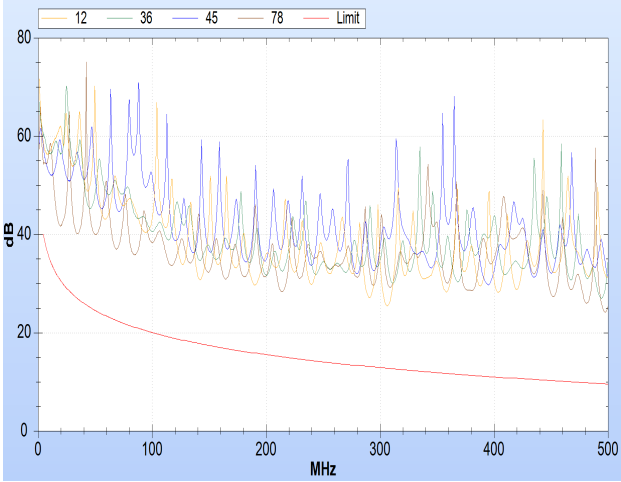

Fig. 11. Transverse Conversion Loss of the complete ETB configuration

Return Loss (RL) is a measure of all reflections that are caused by the impedance mismatches at all locations along the ETB physical layer region. Obviously, a good match between characteristic impedance and termination resistance in the nodes provides for a good transfer of power/data to and from the link and minimize reflections. The return loss measurement varies significantly with frequency. The grey section of the limit line as shown in Figure 10 indicates that the insertion loss (IL) $<$ 3 dB and not evaluated against the test limit (the 3 dB Rule means the integrity of the signal will not be affected below the noise floor or test limit). Sources of return loss are mostly due to variations in the value of the characteristic impedance along the cable and mainly from connectors. Considering the measurements carried out with the field tester, we feel confident that this configuration will perform well, even in a noisy environment such as the harsh railway environment.

Note further that, the test limit line shown in Figures 9 has a low-frequency flat region at 65 dB in the NEXT is often referred to as the measurement plateau. This allows for dynamic range in between the measurement noise floor of the test equipment (either Vector Network Analyzer or field tester) and the limit line. It should be noted that without the plateau, the limit becomes more challenging at low frequency and would cause worse failure. This low-frequency flat region limit line is also applicable to other parameters such as Return Loss at 19 dB and Transverse Conversion Loss at 40 dB and are specified by ISO/IEC JTC1 SC25 WG3 [39] and the TIA TR42.7 committees which form part of the required compliance testing for a given category/class. In the case of the TIA Cat 6A channel test limit, the flat region at the low frequency for the NEXT test limit line is less stringent in comparison to the ISO11801 Channel Class Fa and F test limits.

Figure 11 gives an indication of balance measurement with clear margin between the data points and the test limit to ensure that any noise injected into the cabling is cancelled out. This is accomplished by injecting a differential mode signal into each configuration pair, then measuring the common mode signal returned on that same cabling with a high TCL value means that the impedances of the conductors relative to ground are almost equal. High TCL values correspond to better noise immunity and lower emissions in terms of electromagnetic interference from other sources considering the harsh railway environment. The TCL was not considered as an issue in our previous work [24]. However, the suitability of running the ETB in close proximity with other signal cables was investigated through experimental setups. Generally, the installation of data cabling infrastructure such as twisted-pair copper assembly in close proximity to electrical power cables is anticipated to be susceptible to electromagnetic interference due to harmonics. The resulting effect could adversely disrupt the signal and the communication would become noisy and garbed. In many cases, transmissions will simply not make it. In other cases, transmission rates will slow down as communications are constantly retried. In the event that the data cabling must go near electrical power lines, the norm demands to cross them in perpendicular which was the approach adapted in §II-A with the termination of the imrpoved connectors (e.g., proper shielding to prevent electromagnetic fields from entering or leaving the configuration).

B. ETB experimental results

To validate the ruggedness of our new experimental approach to seamlessly support a 40 Gbit/s link speed over a distance of 55-metres (i.e. length of a passenger car is taken to be 25-metre, a total of 50-metre for the two cars and the inter-car and/or inter-consist is considered to be 5-metre), we use an open-source software known as the Microsoft Network test transmission control protocol (MS NTttcp) [40]. This sends and/or receives a randomly generated data stream from the ETB active nodes through the 40 Gbit/s servers from in-memory buffers, so there is no disk input/output to limit its throughput. This feature makes it a very useful tool for

measuring network performance and throughput analysis. The input parameters are systematically chosen within an allowed set such as Ethernet frame sizes, and optimization of the MS NTttcp software variables to fit the intended application.

As shown in Table IV, the NTttcp optimized variables used for the experiemntal setup are defined as follows; where -l specifies the length of each buffer that NTttcp uses to transfer data, -rb represents the total per-socket buffer space reserved and in turn, controls the receivers transmission control protocol (TCP) window size, -n specifies the number of buffers that NTttcp transfers before it stops and reports the results, -a enables asynchronous data transfer mode, -w directs NTttcp to use Win32 (WSASend and WSARecv) functions to transfer data, -v enables verbose mode, and -fr specifies full receive buffer mode.

TABLE IV
MICROSOFT NTTTCP SOFTWARE INPUT PARAMETERS SETTINGS FOR THE TESTBED

Transmitting server/switch setting		Receiving server/switch setting	
-l	1048576	-l	1048576
-rb	N/A	-rb	220000
-n	100000	-n	100000
-a	16	-a	16
-w	No value	-w	No value
-v	No value	-v	No value
-fr	No value	-fr	No value

Taking into consideration the maximum transmission unit (jumbo frame) [41] and [42] used in this experimental setup, the overall output results are shown in Table V using the NTttcp software to realise end-to-end 40 Gbit/s throughput clearly demonstrates the robustness and reliability of our new approach over standard RailCat cabling and enhanced connector with minimum retransmission or no errors. This suggests that the link speed is approximately 40 Gbit/s over four 10 Gbit/s links. The number of packets sent and packets received in bytes, as shown in Table V for both outputs are in good correlation. The retransmission rate is calculated either in terms of segments or bytes but in this study, the latter was chosen and the byte retransmission rate was evaluated to be less than 1.0 % in accordance with [43].

TABLE V
SUMMARY TEST RESULTS OF USING MICROSOFT NTTTCP BENCHMARK SOFTWARE TO VALIDATE 40 GBIT/S THROUGHPUT OVER THE RAILCAT CABLING/ENHANCED CONNECTORS CONFIGURATION

Tx. outputs		Rx outputs	
Total Bytes (Mega)	415146.97	Total Bytes (Mega)	415197.30
Realtime (s)	84.69	Realtime (s)	86.70
Frame Size (Bytes)	9000	Frame Size (Bytes)	9000
Total Throughput (Mbit/s)	39214.75	Total Throughput (Mbit/s)	38310.73
Packet sent (Bytes)	**46339108**	Packet sent (Bytes)	**1959051**
Packet received (Bytes)	**1959120**	Packet received (Bytes)	**46339056**
Total retransmits	22	Total retransmits	0
Total errors	0	Total errors	0

IV. CONCLUSIONS

In this paper, we demonstrated the benefits of RailCat 5e twisted-quad copper cabling for the ETB physical layer region consisting of inter-car and/or inter-consist, advanced rail-approved ETBNs and connectors assemblies for higher data transmission in the harsh railway environment for the targeted application of ETB communication systems with no error and an insignificant retransmission rate. With this new approach, train operating companies can reliably support traffic on-board trains up to the level of 5G and beyond communication systems to enhance passengers' level of experience and expectations, increase take-up, improve predictive and preventive maintenance leading to reductions in operational expenditure due to downtime. The achievable data rate 40 Gb/s using this method exceeds the current internationally specified standards, referenced in [6] by up to 90 percent. This approach is pushing the frontiers of knowledge, and it is expected that the referenced industry standards will be revised to accommodate higher capacity in the near future.

Future direction of this research would focus on exploring cutting-edge wireless technologies, specifically the IEEE 802.11ax [44] and IEEE 802.11be [45] standards. The objective is to further advance seamless Train-to-Shore connectivity, achieving gigabit throughput-per-area in high-density scenarios while extending the range and bolstering the resilience of backbone to service diversity.

ACKNOWLEDGMENT

The authors wish to express their gratitude to Mr. Nick Warren, a research technician at the School of Computer Science Electronic and Engineering, University of Essex, for his invaluable technical assistance. Additionally, the authors extend their appreciation to the LPA assembly and engineering team for their contributions to the construction of the 40 Gbit/s throughput guided media configuration. Finally, the authors would like to thank the anonymous reviewers and the associate editor for their valuable comments and suggestions, which played a pivotal role in enhancing the quality of the paper to its current state.

REFERENCES

[1] C. Schifers and G. Hans, "IEC 61375-1 and uic 556-international standards for train communication," in *VTC2000-Spring. 2000 IEEE 51st Vehicular Technology Conference Proceedings (Cat. No. 00CH37026)*, vol. 2. IEEE, 2000, pp. 1581–1585.

[2] H. Kirrmann and P. A. Zuber, "The iec/ieee train communication network," *IEEE Micro*, vol. 21, no. 2, pp. 81–92, 2001.

[3] Electronic railway equipment - Train Communication Network (TCN), "IEC 61375-1:2012-06 - Part 1: General architecture," 2012-06. [Online]. Available: https://webstore.iec.ch/

[4] ——, "IEC 61375-3-1:2012-06 - Part 3-1: Multifunction Vehicle Bus (MVB)," 2012-06. [Online]. Available: https://webstore.iec.ch/5398

[5] ——, "IEC 61375-2-1:2012-06 - Part 2-1: Wire Train Bus (WTB)," 2012-06. [Online]. Available: https://webstore.iec.ch/5398

[6] ——, "IEC 61375-2-5 ETB (Ethernet Train Backbone)," 2014-08. [Online]. Available: https://webstore.iec.ch/publication/5400

[7] ——, "IEC 61375-3-4 ECN (Ethernet Consist Network)," 2014-03. [Online]. Available: https://webstore.iec.ch/publication/5405

[8] K. Guan, G. Li, T. Kürner, A. F. Molisch, B. Peng, R. He, B. Hui, J. Kim, and Z. Zhong, "On millimeter wave and THz mobile radio channel for smart rail mobility," *IEEE Transactions on Vehicular Technology*, vol. 66, no. 7, pp. 5658–5674, 2016.

[9] J. Kim, M. Schmieder, M. Peter, H. Chung, S.-W. Choi, I. Kim, and Y. Han, "A comprehensive study on mmwave-based mobile hotspot network system for high-speed train communications," *IEEE Transactions on Vehicular Technology*, vol. 68, no. 3, pp. 2087–2101, 2018.
[10] F. Hasegawa, A. Taira, G. Noh, B. Hui, H. Nishimoto, A. Okazaki, A. Okamura, J. Lee, and I. Kim, "High-speed train communications standardization in 3GPP 5G NR," *IEEE Communications Standards Magazine*, vol. 2, no. 1, pp. 44–52, 2018.
[11] J. Gozalvez, "5G worldwide developments [mobile radio]," *IEEE Vehicular Technology Magazine*, vol. 12, no. 1, pp. 4–11, 2017.
[12] M. Mueck, E. C. Strinati, I.-G. Kim, A. Clemente, J.-B. Dore, A. De Domenico, T. Kim, T. Choi, H. K. Chung, G. Destino *et al.*, "5G CHAMPION-Rolling out 5G in 2018," in *2016 IEEE Globecom Workshops (GC Wkshps)*. IEEE, 2016, pp. 1–6.
[13] S. E. Dudley, T. J. Quinlan, and S. D. Walker, "1.6 Gb/s data throughput optically-remoted leaky feeders for underground transport environments," in *Vehicular Technology Conference, 2007. VTC2007-Spring. IEEE 65th*. IEEE, 2007, pp. 520–524.
[14] B. Ai, K. Guan, M. Rupp, T. Kurner, X. Cheng, X.-F. Yin, Q. Wang, G.-Y. Ma, Y. Li, L. Xiong *et al.*, "Future railway services-oriented mobile communications network," *IEEE Communications Magazine*, vol. 53, no. 10, pp. 78–85, 2015.
[15] D. T. Fokum and V. S. Frost, "A survey on methods for broadband internet access on trains," *IEEE communications surveys & tutorials*, vol. 12, no. 2, pp. 171–185, 2010.
[16] G. Shafiullah, A. Gyasi-Agyei, and P. Wolfs, "Survey of wireless communications applications in the railway industry," in *Wireless Broadband and Ultra Wideband Communications, 2007. AusWireless 2007. The 2nd International Conference on*. IEEE, 2007, pp. 65–65.
[17] K. Yang, M. Berbineau, J.-P. Ghys, Y. Cocheril, and D. Seetharamdoo, "Propagation measurements with regional train at 60 GHz for virtual coupling application," in *Antennas and Propagation (EUCAP), 2017 11th European Conference on*. IEEE, 2017, pp. 126–130.
[18] Y. Ghasempour, C. R. da Silva, C. Cordeiro, and E. W. Knightly, "IEEE 802.11 ay: Next-generation 60 GHz communication for 100 Gb/s Wi-Fi," *IEEE Communications Magazine*, vol. 55, no. 12, pp. 186–192, 2017.
[19] J. Goikoetxea, S. Tesar, A. Heindel, G. Hans, V. Mayeux, A. Grasso, M. U. Colera, and I. Lopez, "Shift2Rail CONNECTA Deliverable D8.3 – Final Report on the Contribution of CONNECTA to Shift2Rail. Shift2Rail CONNECTA," pp. 13–14, 2018.
[20] S. Ahamed, "Visible light communication in railways," *IET*, 2016.
[21] G. Barbu, "E-train-broadband communication with moving trains," *International Union of Railways*, 2010.
[22] M. Aguado, O. Onandi, P. Agustin, M. Higuero, and E. Taquet, "WiMax on rails," *IEEE Vehicular Technology Magazine*, vol. 3, no. 3, pp. 47–56, 2008.
[23] C.-H. Yeh, C.-W. Chow, Y.-L. Liu, S.-K. Wen, S.-Y. Chen, C.-R. Sheu, M.-C. Tseng, J.-L. Lin, D.-Z. Hsu, and S. Chi, "Theory and technology for standard WiMAX over fiber in high speed train systems," *Journal of Lightwave Technology*, vol. 28, no. 16, pp. 2327–2336, 2010.
[24] F. Ngobigha, S. D. Walker, G. Koczian, G. Howell, and J. Prentice, "Demonstration of 40 Gbit/s conducting media data capacity on international rolling stock." in *WONS*, 2019, pp. 154–157.
[25] D. Barnett, D. Groth, and J. McBee, *Cabling: the complete guide to network wiring*. John Wiley & Sons, 2006.
[26] J. A. Stratton, *Electromagnetic theory*. John Wiley & Sons, 2007.
[27] A. Oliviero and B. Woodward, *Cabling: the complete guide to copper and fiber-optic networking*. John Wiley & Sons, 2014.
[28] C. Spurgeon, *Ethernet: the definitive guide*. " O'Reilly Media, Inc.", 2000.
[29] K. M. Ramachandran and C. P. Tsokos, *Mathematical statistics with applications in R*. Academic Press, 2020.
[30] D. Albalate, G. Bel, and X. Fageda, "Competition and cooperation between high-speed rail and air transportation services in europe," *Journal of transport geography*, vol. 42, pp. 166–174, 2015.
[31] J. D. Jackson, "Classical electrodynamics," 1999.
[32] P. H. Dawson, *Quadrupole mass spectrometry and its applications*. Elsevier, 2013.
[33] E. De Hoffmann, "Mass spectrometry," *Kirk-Othmer Encyclopedia of Chemical Technology*, 2000.
[34] R. E. March, "An introduction to quadrupole ion trap mass spectrometry," *Journal of mass spectrometry*, vol. 32, no. 4, pp. 351–369, 1997.
[35] P. Nystedt, "A proof of the law of sines using the law of cosines," *Mathematics Magazine*, vol. 90, no. 3, pp. 180–181, 2017.
[36] D. Agarwal, *Tensor Calculus and Riemannian Geometry*. Krishna Prakashan Media, 2013.
[37] M. Schwartz, *Principles of electrodynamics*. Courier Corporation, 2012.
[38] F. H. Read, "Electromagnetic radiation," *Chichester, Sussex, England and New York, John Wiley and Sons, 1980. 344 p*, 1980.
[39] Cabling, Customer Premises, "ISO/IEC JTC 1/SC 25/WG 3," *Def*, vol. 10, p. 14, 2008.
[40] Microsoft Network test transmission control protocol, "NTttcp Utility: Profile and Measure Windows Networking Perormance," 2016. [Online]. Available: https://gallery.technet.microsoft.com
[41] P. Prakash, M. Lee, Y. C. Hu, R. R. Kompella *et al.*, "Jumbo frames or not: That is the question!" 2013.
[42] K. Sharma and V. Badarla, "Curtailing latency in data center network by adopting jumbo frames," in *2016 IEEE International Conference on Advanced Networks and Telecommunications Systems (ANTS)*. IEEE, 2016, pp. 1–6.
[43] H.-K. Kahng, *Information Networking: Networking Technologies for Enhanced Internet Services, International Conference, ICOIN 2003, Cheju Island, Korea, February 12-14, 2003, Revised Selected Papers*. Springer, 2003, vol. 2662.
[44] E. Khorov, A. Kiryanov, A. Lyakhov, and G. Bianchi, "A tutorial on ieee 802.11 ax high efficiency wlans," *IEEE Communications Surveys & Tutorials*, vol. 21, no. 1, pp. 197–216, 2018.
[45] E. Khorov, I. Levitsky, and I. F. Akyildiz, "Current status and directions of ieee 802.11 be, the future wi-fi 7," *IEEE access*, vol. 8, pp. 88 664–88 688, 2020.

Felix Ngobigha received the B.Tech. (Hons.) degree in electrical engineering with a focus on electronics from the Rivers State University of Science & Technology in Port Harcourt, Nigeria, in 2000, the MSc. in telecommunications & information systems, followed by a PhD in computing and electronic systems, both of which he completed at the University of Essex in Colchester, UK, in 2005 and 2015, respectively.

From 2001 to 2004, he held the position of a Scientific Officer at the Centre for Satellite Technology Development, which was affiliated with the National Space Research and Development Agency in Abuja, Nigeria. During this time, he collaborated with Surrey Satellite Technology Limited in Guildford, UK, contributing to the development and launch of the NigeriaSat-1 microsatellite for disaster monitoring - remote sensing applications. Between 2004 and 2011, he served as a Lecturer at the Department of Electrical/Electronics Engineering at Niger Delta University in Nigeria. Subsequently, from 2016 to 2020, he assumed the role of a Postdoctoral Researcher at the School of Computer Science and Electronic Engineering at the University of Essex, UK. He joined the University of Suffolk, UK in 2020 initially as a Lecturer and promoted to Senior Lecturer in 2023. Currently, he serves as the Technology Lead for the Networking and Security Technologies theme within the Digital Futures Institute (DFI) and fulfills the role of Course Leader for MSc Advanced Computing. Over the course of his career, he has actively participated in various projects, including those sponsored by the European Union (EU) and Innovate UK, in addition to collaborative endeavors bridging academia and industry. He has made significant contributions to numerous peer-reviewed journals and conference papers. His diverse research interests cover a broad spectrum of topics, such as future networks, IoT security, machine learning applications in communications, electromagnetic propagation and scattering with applications in weather radar and remote sensing, microwave and antenna theory, as well as advanced digital and analogue electronic designs.

Geza Koczian was awarded an MSc. by research in multi-mode transmission line propagation at Essex University in 2012.

He then joined the Access Network Group at Essex University. Since then he has been involved in a number of EPSRC, Innovate UK and EU funded projects, and has published several journal and refereed conference papers. He was responsible for the design and realization of the first 10GbE backbone system for trains as part of a Knowledge Transfer Partnership in 2013.

Stuart D. Walker was born in Dover, U.K in 1952. He received the B.Sc. (Hons) degree in physics from Manchester University, Manchester, U.K., in 1973, the M.Sc. degree in telecommunications systems and Ph.D. degree in electronics from Essex University, Colchester, U.K., in 1975 and 1981 respectively.

From 1981-82, he was a post-doctoral research assistant at Essex University. From 1982-87, he was a research scientist at BT Research Lab, and from 1987-88 he was promoted to Group Leader in Submarine Systems Design. He joined Essex University in 1988 as a Senior Lecturer, and was promoted to Reader in 2002 and to Full Professor in 2004. At Essex University, he manages a laboratory concerned with all aspects of Access Networks: the Access Networks Group (ANG). Prof. Walker been involved in many EPSRC and European Union research projects over the years, recent examples being: e-Photon-I and II, BONE, MUSE-I and II, UROOF, STRONGEST, FIVER, OASE, SODALES, NIRVANA, iCirrus and CHARISMA. Much of the EU project work has involved remote collaboration with colleagues across mainland Europe. The ANG has developed a complete and affordable 8K UHDTV set-up, which uses an in-house designed, state-of-the art, video codec. 4K UHDTV is compressed to just 8 Mbit/s on average (a world-class performance).This was featured in a live 4K webcast of a University of Essex graduation: http://vase.essex.ac.uk/projects/streaming-uhd/index.html. More recently, 8K UHDTV data has been compacted to a typical 100 Mbit/s data-rate using new correlation-based workflows to beat the expected 128 (16 x 8) Mbit/s requirement. These video collaboration technologies use affordable subsystems and are scalable to higher resolutions (e.g. 16K); making the technology future-proof. Live 4K video capture is available in-house whilst 8K cameras are now becoming affordable. Railway communications technology has also featured in the ANG portfolio culminating with the commercial deployment 10 GbE backbones for trains in a knowledge – transfer partnership; an impact cited in the University's REF 2020 submission. A complete 2 kW sound system (including loudspeakers) has been funded by Essex University to support the ANG's research into remote collaboration and telepresence.